Research Article

SURFACE and INTERFACE ANALYSIS

Received: 11 October 2010 Revised: 27 February 2011 Accepted: 2 March 2011 Published online in Wiley Online Library:

(wileyonlinelibrary.com) DOI 10.1002/sia.3766

New insights into the Sn underpotential deposition on Au(100)

L. A. Meier, S. G. García and D. R. Salinas*

The underpotential deposition (UPD) of Sn in the system Au(100)/Sn^{2+}, SO_4^{2-} has been studied by classical electrochemical techniques and *in situ* scanning tunneling microscopy. The results show that the Sn UPD initiates at relatively high potentials with the formation of a quasi-hexagonal structure characterized as Au(100) − ($\sqrt{2} \times 7$)R45°. This expanded overlayer contributes to the modification of the surface morphology which exhibits flat terraces with step edges showing angles of 60 or 120°. At lower potentials two-dimensional (2D) islands are formed which tend to grow, causing a coverage increase. In the underpotential region close to the formation of the 3D bulk phase the long time polarization experiments indicate the formation of different Au–Sn alloy phases.

Keywords: Sn; UPD; Au(100); STM

Introduction

The formation of metal monolayers or submonolayers onto a foreign metal surface is a classical research topic in interfacial electrochemistry because some of these modified surfaces have electrocatalytic or catalytic properties better than those of the pure components.[1] This type of ultrathin films can be electrochemically obtained by underpotential deposition (UPD) or overpotential deposition (OPD), as the coverage of metal deposits from submonolayers upto several monolayers can be well adjusted through charge measurements. For instance, the UPD process of different metals on well-characterized single crystal surfaces such as Au(*hkl*), and also polycrystalline gold, has been widely studied.[2] This is not the case of the system Au/Sn^{2+} which has received little attention, and only a few works related to the UPD process were reported.[3–8] Regarding the Sn UPD on gold single crystals, Mao *et al*.[6] studied the structure and dynamics of Sn UPD on unreconstructed and reconstructed Au(111) surface by *in situ* scanning tunneling microscopy (STM). They concluded that on the unreconstructed Au(111) surface Sn forms very small size-controlled two-dimensional (2D) clusters which, subsequently, immerse into the substrate surface forming surface alloying at low underpotentials. On the other hand, on the reconstructed surface, Sn nucleates in the face-centered cubic regions following an anisotropic growth owing to the underneath reconstruction of the bare Au surface. Also in this case, Sn forms a surface alloy with the substrate at low underpotentials. The UPD of Sn on Au(100) was also studied by Mao *et al*.[7] and based on the topographic changes observed by scanning tunneling microscopy they concluded that the process proceeds in three stages: the initial formation of a submonolayer, surface alloying, and finally the formation of a bulk alloy.

In this paper, we describe new results concerning the initial stages of the Sn electrodeposition process on Au(100). The possibility of surface alloying during this process is also discussed.

Experimental

The experiments were carried out in the systems Au(100)/0.5 M H_2SO_4 and Au(100)/1 mM $SnSO_4$ + 0.5 M H_2SO_4 at a temperature T = 298 K. The electrolytic solutions were prepared from suprapure chemicals (Merck, Darmstadt) and fourfold quartz-distilled water. Prior to each experiment the solutions were deaerated by nitrogen bubbling.

The working electrode was a Au(100) single crystal (diameter $\emptyset$ = 0.4 cm). The surface was first mechanically polished with diamond paste of decreasing grain size down to 0.25 μm and subsequently electrochemically polished in a cyanide bath according to a standard procedure.[9] Classical electrochemical studies were performed in a standard three-electrode electrochemical cell. A platinum sheet (1 cm^2) was used as a counter electrode and a $Hg/Hg_2SO_4/K_2SO_4$ saturated electrode (SSE) served as a reference electrode. All potentials in this study are referred to the SSE. The measurements were carried out with a potentiostat–galvanostat EG&G Princeton Applied Research Model 273A.

A standard Nanoscope III equipment (Digital Instruments, Santa Barbara, CA, USA) was used for the *in situ* STM studies, employing Apiezon insulated Pt–Ir tips. Pt wires served as counter and quasi-reference electrodes. The potentials of the gold substrate and the STM tip were controlled independently by a Nanoscope III-bipotentiostat optimized for the STM setup used. The tip potential was held constant at a value of minimum faradaic current and the tip current varied in the range $2 \leq I_{tun}/nA \leq 20$.

Results and Discussion

Figure 1 shows typical cyclic voltammograms obtained for the systems Au(100)/SO_4^{2-} and Au(100)/Sn^{2+}, SO_4^{2-}. For the Sn^{2+} free solution, the steady-state cyclic voltammogram obtained after

* *Correspondence to: D. R. Salinas, Departamento de Ingeniería Química, Instituto de Ingeniería Electroquímica y Corrosión (INIEC), Universidad Nacional del Sur, Avda. Alem 1253, (8000) Bahía Blanca, Argentina.*
E-mail: dsalinas@uns.edu.ar

Departamento de Ingeniería Química, Instituto de Ingeniería Electroquímica y Corrosión (INIEC), Universidad Nacional del Sur, Avda. Alem 1253, (8000) Bahía Blanca, Argentina

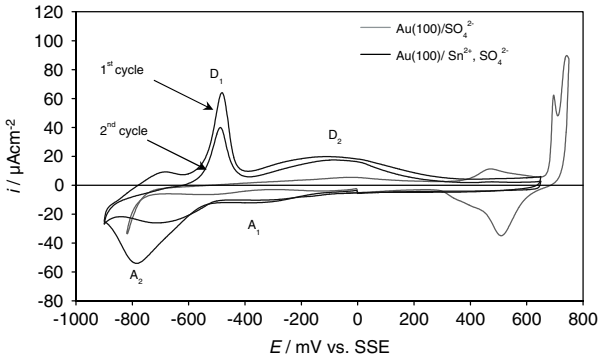

Figure 1. Cyclic voltammograms of Au(100) in 0.5 M H_2SO_4 solution (———) and in 1 mM $SnSO_4$ + 0.5 M H_2SO_4 solution (——). $|dE/dt| = 50\ mV\ s^{-1}$.

several cycles shows the typical and very extensive double layer region of the substrate. The cathodic current density increase recorded at $E = -750$ mV and the anodic peaks registered at $E \geq 650$ mV correspond to the hydrogen evolution reaction and the substrate oxidation, respectively. The characteristic anodic peak related to the lifting of surface reconstruction[10] is absent, denoting that a Au(100) − (1 × 1) surface is present in the potential range analyzed. According to Hamelin,[11] the atomic superficial structure is sensitive to the surface preparation. Thus, the mechanical polishing, the electrochemical treatment or the flame annealing conditions used to prepare the surface affect its initial surface atomic structure. For example, a predominantly reconstructed surface is only present in flame annealed surfaces cooled in air. Other surface treatments or cooling conditions after the flame annealing produce predominantly unreconstructed or partially reconstructed surfaces. Considering the equilibrium potential of the 3D Sn phase ($E_{3DSn} = -880$ mV) for the Sn^{2+} containing solution, the Sn UPD is clearly observed during the cathodic sweep in the potential range $-880\ mV \leq E \leq 0.0\ mV$, where a broad shoulder A_1 and a peak A_2 are recorded. The presence of Sn on the substrate is also evidenced by the inhibition of the H_2 evolution reaction at the cathodic end. During the anodic sweep two stages of desorption are identified, through the anodic peak D_1 ($-600\ mV \leq E \leq -400\ mV$) followed by a broad peak, D_2, that extends until the potential at which the substrate oxidation begins. The repetitive potential cycling in this UPD region generates voltammograms that vary with the number of cycles, indicating the existence of irreversible phenomena associated with the adsorption of Sn, probably related to the formation of an Au–Sn alloy.

The changes in the surface morphology during the initial stages of Sn UPD in the system Au(100)/Sn^{2+}, SO_4^{2-} were followed by *in situ* STM analysis. At potentials $E \geq 300$ mV it can be assumed that the Au(100) surface is nearly free of Sn. The surface consists of atomically smooth terraces with rounded edges separated by monatomic steps (Fig. 2(a)). Only a high surface mobility is observed ('frizzy steps') which produces morphological changes of the flat terraces. When the potential is changed to $E = 250$ mV (Fig. 2(b)) lateral growth of the terraces from the edges is verified, and the rounded edges of the terraces take on a distinctly different morphology, showing angles of 60 or 120°. This effect is more evident at $E = 150$ mV where the growth of some terraces is even greater (Fig. 2(c)). Modifying the potential to more negative values there is a new structural change in the terraces with the appearance of 2D islands that tend to further increase the coverage

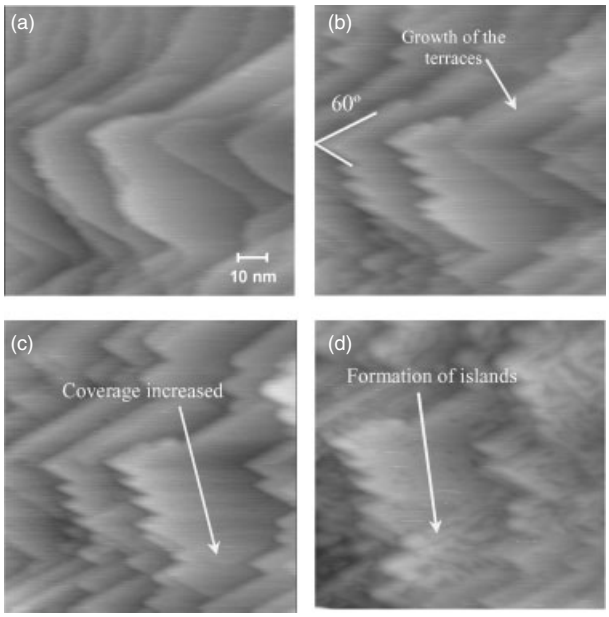

Figure 2. Sequence of *in situ* STM images obtained in the system Au(100)/Sn^{2+}, SO_4^{2-} at (a) $E = 550$ mV; (b) $E = 250$ mV, polarization time $t_p = 360$ s; (c) $E = 150$ mV, $t_p = 270$ s; (d) $E = -50$ mV, $t_p = 180$ s.

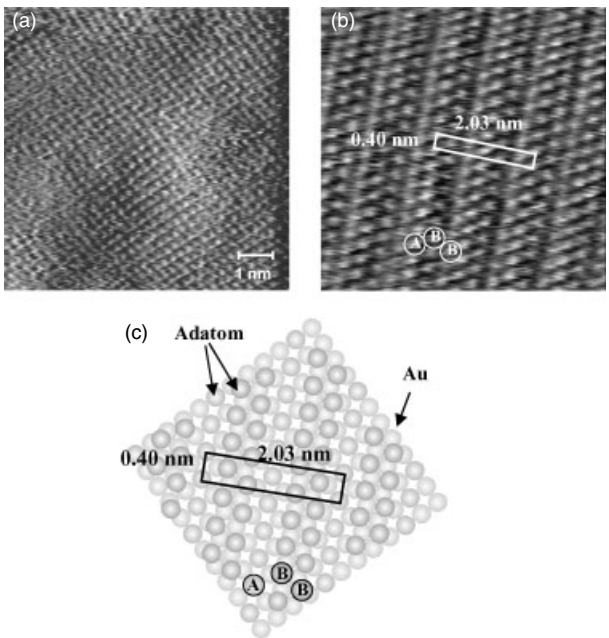

Figure 3. *In situ* STM images with lateral atomic resolution in the system Au(100)/Sn^{2+}, SO_4^{2-}, at (a) $E = 550$ mV; (b) $E = 100$ mV; (c) model for the overlayer structure shown in (b).

(Fig. 2(d)). At potentials values $E < -400$ mV the images quality were lost due to an increased deposition rate.

Images with atomic resolution obtained at $E = 550$ mV (Fig. 3(a)) showed a 2D quadratic lattice with an interatomic spacing of 0.29 ± 0.02 nm, which corresponds to the atomic structure of the unreconstructed Au(100) surface free of Sn deposits. In the potential range $50\ mV \leq E \leq 250\ mV$, an expanded quasi-hexagonal lattice is recorded (Fig. 3(b)), which gives rise to 60° angles at the edges of the terraces. Figure 3(a)

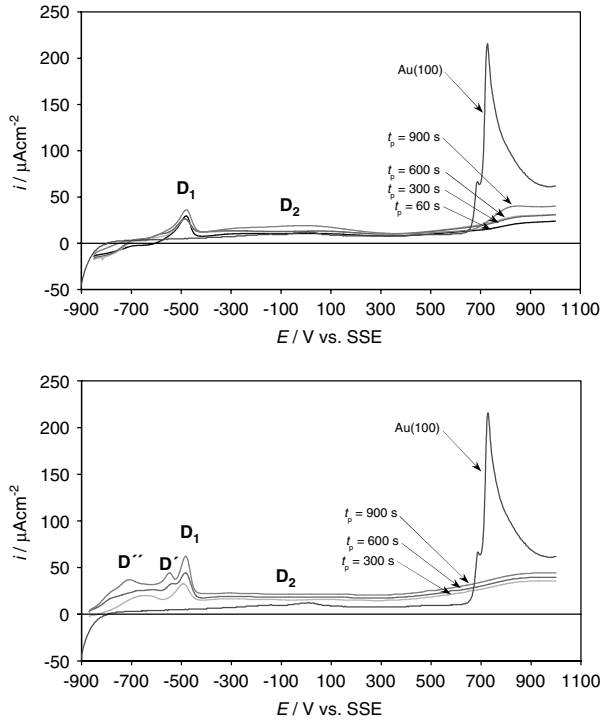

Figure 4. Anodic stripping curves obtained in the system Au(100)/Sn^{2+}, SO_4^{2-} after different polarization times at (a) $E_k = -850$ mV, (b) $E_k = -870$ mV. $|dE/dt| = 50$ mV s^{-1}.

and (b) are results of the same STM experiment, and, therefore, it is possible to compare them in order to typify the quasi-hexagonal superlattice. This overlayer is characterized by two types of parallel rows, formed by brighter spots 'A' and darker spots 'B', respectively. These rows are rotated by 45° with respect to the [0,0,1] atomic rows of the Au(100) substrate. The spacing between the spots is 0.39 ± 0.02 nm. Considering these data the quasi-hexagonal structure can be denoted as Au(100) $-(\sqrt{2} \times 7)$R45° and is shown schematically in Fig. 3(c). The characteristics of this structure and the potential range where it was recorded suggest that it is not related to the Au substrate surface reconstruction. Moreover, the increased surface coverage when the potential is less positive indicates that this structure is related to the UPD of Sn, although no adsorption peaks are observed in the voltammogram in this potential range. Nevertheless, taking into account the results presented by Rodes *et al*.[12] for the irreversible adsorption of Sn on Au(hkl) the anions may be involved in the tin adlayer. Thus, the expanded metal superlattice structure observed in this work can be stabilized by coadsorbed anions.[13] For example, the honeycomb structure Au(111) $-2(\sqrt{3} \times \sqrt{3})$R30°Cu is stabilized by cosorption of HSO_4^- at the centers of the honeycombs. The cosorption of anions was also suggested during the Ag UPD on Au(100)[14] and an expanded quasi-hexagonal Ag structure similar to that showed in Fig. 3 was also reported.

In order to investigate the irreversible phenomena observed in the voltammograms of Fig. 1 long time polarization experiments were performed. The potential was stepped from $E = 550$ mV, i.e. a potential value where no Sn adsorption was observed, to different potentials, E_k, close to the equilibrium potential of the 3D Sn phase. After maintaining the selected E_k value for different polarization times, t_p, the potential was swept back recording the corresponding $E - i$ desorption spectra (Fig. 4). After the polarization at $E_k = -850$ mV practically no variations in the peaks D_1 and D_2 are observed and the corresponding charges do not show changes with t_p. Nevertheless, in both cases, the peaks corresponding to the substrate oxide formation are affected. The Au(100) surface is disordered during the Sn adsorption process perhaps by the formation of an Au–Sn alloy, which is removed during the anodic scan.[12,15] Considering that peaks D_1 and D_2 are not strongly distorted, this alloy process probably follows a place exchange mechanism between Sn atoms and Au surface atoms, affecting only the firsts Au layers.[16–18] However, at $E_k = -870$ mV a significant formation of surface alloy is observed which is reflected in the anodic stripping curves. The charges corresponding to peaks D_3 and D_4 increased with t_p and, in addition, new anodic peaks D′ (-600 mV $\leq E \leq -530$ mV) and D″0 (-780 mV $\leq E \leq -650$ mV) are recorded. The stripping charge density, Δq, increases significantly for $t_p = 900$ s ($\Delta q_{exp} \approx 1600$ μC cm^{-2}) exceeding that required for the deposition of an Sn monolayer ($\Delta q_{mon} = 770$ μC cm^{-2}). These results can be attributed to the formation of different 3D Sn–Au alloy phases, evidenced by the presence of the additional stripping peaks D′ and D″. Therefore, further work is required to analyze in more detail the mechanism of the alloy formation process observed in this system. Additionally, the anions adsorbed on the gold surface could influence the formation of the superlattice structure. These studies are now in progress.

Conclusions

The UPD process of Sn on Au(100) was examined by classical electrochemical techniques and *in situ* STM. The STM images indicated that the deposition of Sn onto the Au(100) surface initiates at relatively high potentials with the formation of an expanded adlayer with a superlattice structure Au(100) $-(\sqrt{2} \times 7)$R45°. This structure contributes to the modification of the surface morphology which exhibits flat terraces with edges showing angles of 60 or 120°. At more negative potential values there is a new structural change in the terraces with the appearance of 2D islands that tend to further increase the coverage. At potentials close to the 3D Sn phase, the long time polarization experiments indicate the formation of Au–Sn alloy phases.

Acknowledgements

The authors wish to thank the Universidad Nacional del Sur, Argentina, for the financial support of this work. L. A. Meier acknowledges a fellowship granted by CONICET.

References

[1] N. M. Marković, P. N. Ross Jr, *Surf. Sci. Rep.* **2002**, *45*, 117.
[2] E. Herrero, L. J. Buller, H. D. Abruña, *Chem. Rev.* **2001**, *101*, 1897.
[3] V. A. Vicente, S. Bruckenstein, *Anal. Chem.* **1972**, *44*, 297.
[4] I. Petersson, E. Ahlberg, *J. Electroanal. Chem.* **2000**, *485*, 178.
[5] M. Fonticelli, R. I. Tucceri, D. Posadas, *Electrochim Acta.* **2004**, *49*, 5197.
[6] B. W. Mao, J. Tang, R. Randler, *Langmuir* **2002**, *18*, 5329.
[7] J. W. Yang, J. Tang, Y. Y. Yang, J. M. Wu, Z. X. Xie, S. G. Sun, B. W. Mao, *Surf. Interface Anal.* **2001**, *32*, 49.
[8] L. A. Meier, *Desarrollo de sistemas bi- o tri-metálicos conpropiedades catalíticas para el tratamiento electroquímico de efluentes contaminados con iones nitrato*, Ph.D. Thesis, Universidad Nacional del Sur, Argentina, **2010**.
[9] K. Engelsmann, W. J. Lorenz, E. Schmidt, *J. Electroanal. Chem.* **1980**, *114*, 1.

[10] A. Hamelin, *J. Electroanal. Chem.* **1995**, *386*, 1.
[11] A. Hamelin, *J. Electroanal. Chem.* **1996**, *104*, 1.
[12] A. Rodes, E. Herrero, J. M. Feliu, A. Aldaz, *J. Chem. Soc. Faraday Trans.* **1996**, *92*, 3769.
[13] E. Budevski, G. Staikov, W. J. Lorenz, *Electrochemical Phase Formation and Growth – An Introduction to the Initial Stages of Metal Deposition*, VCH: Weinheim, **1996**.
[14] S. García, D. Salinas, C. Mayer, E. Schmidt, G. Staikov, W. J. Lorenz, *Electrochim. Acta* **1998**, *43*, 3007.
[15] L. A. Meier, D. R. Salinas, J. M. Feliu, S. G. García, *Electrochem. Commun.* **2008**, *10*, 1583.
[16] M. C. del Barrio, S. G. García, D. R. Salinas, *Electrochem. Commun.* **2004**, *6*, 762.
[17] S. G. García, D. R. Salinas, G. Staikov, *Surf. Sci.* **2005**, *576*, 9.
[18] G. Staikov, S. G. García, D. R. Salinas, *ECS Transactions* **2010**, *25*, 3.